

A Detailed Study of the GG Tau Circumbinary Disk

Caer-Eve McCabe & Andrea M. Ghez

UCLA Division of Astronomy and Astrophysics, Los Angeles CA
90095-1562, USA

Abstract. We present near-infrared images of the circumbinary disk surrounding the pre-main-sequence binary star, GG Tau A, obtained with NICMOS aboard the Hubble Space Telescope. These images have a SNR ~ 25 times higher than previous ground-based measurements, which allows the spatially resolved disk to be explored in detail. The geometry of the ring implies that the circumbinary disk is not intrinsically circular, possibly due to interactions with the central binary star. Overall, the circumbinary disk is redder than the central binary, with the amount of red excess increasing with wavelength. Significant variations in color over the 13 arcsec^2 covered by the disk are also observed, raising the possibility that disk inhomogeneities are present.

1. Introduction

GG Tau is one of the few T Tauri stars whose disk has been imaged at both millimeter and near-infrared wavelengths and is therefore an ideal system for the study of disk material. The massive ($0.13 M_{\odot}$, Guilloteau et al. 1999) disk surrounds a central binary star, whose components are separated by $0.''25$ (37 AU at $d = 147 \text{ pc}$, Bertout et al. 1999). Originally detected in thermal emission at millimeter wavelengths (Simon & Guilloteau 1992; Dutrey et al. 1994) the disk was subsequently observed in near-infrared scattered light in deconvolved adaptive optics (AO) images (Roddier et al. 1996); the disk was observed as a complete ring at H ($1.65 \mu\text{m}$) and only a partial ring at J ($1.25 \mu\text{m}$) and K ($2.2 \mu\text{m}$). Analysis of the near-infrared images offered two particularly intriguing results. First, unusual colors for the integrated disk compared to the central binary were derived, although the uncertainties are large ($E(J-H) = 0.65 \pm 0.32$, $E(H-K) = -0.34 \pm 0.45$). Second, putative 'streamers' of material connecting the disk and the central binary were identified, which, if real, raise interesting possibilities for feeding of the inner circumstellar disks. In order to study the circumbinary disk's colors and the streamers in greater detail, we have carried out a high resolution near-infrared imaging program with the Hubble Space Telescope (HST). Space-based observations such as these offer a more stable point spread function (PSF) which is critical to the detection and characterization of the extended emission.

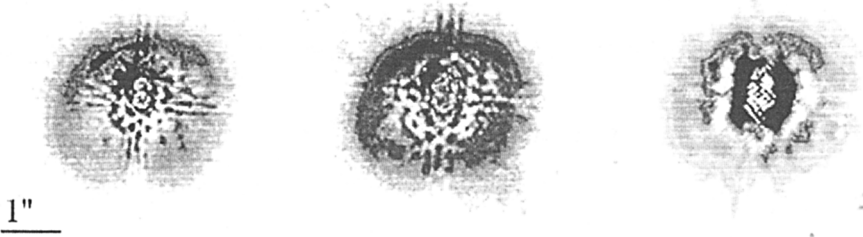


Figure 1. PSF subtracted NICMOS images for the filters F110W (left), F160W (middle) and F205W (right). North is up and east to the left in these images. Although PSF subtraction noise dominates the central regions, the circumbinary disk is clearly observable at radii of $\sim 1''$.

2. Disk Detection & Morphology

In order to estimate the properties of the circumbinary disk, models of the central binary, obtained by PSF fitting, are subtracted from the images. The nine observations at each wavelength allow us to construct both average maps (see Figure 1) and standard deviation maps. The circumbinary disk is easily detected at radii greater than $\sim 1''$ at all three wavelengths, with a disk peak surface brightness of 15.2, 14.0 and 13.4 mag/arcsec² in F110W, F160W and F205W, respectively. At smaller radii the 1σ noise level rises dramatically and dominates (SNR < 3 per pixel) at radii less than $0.''8$; therefore, although the SNR of our disk detection is a factor of ~ 25 higher than that of Roddier et al. (1996), we are unable to detect the streamers in the region between the circumbinary disk and the central stars.

A model of the two-dimensional disk geometry is constructed by analyzing the intensity profile of the disk as a function of azimuth. For every 10 degree segment of the disk an average radial profile is produced. Both the peak intensity and width vary azimuthally in a correlated way. The disk intensity decreases by a factor of ~ 2 from the North side to the South side, whereas the disk width increases by a factor of ~ 2 . Roddier et al. (1996) also saw the intensity variation and suggested that this could be explained by the difference between forward and backward scattering from the dust particles in the disk. Width variations in the disk may also be due to the form of the dust particles phase function and/or to geometric effects. The inclination and shape of the disk is explored by fitting the intensity peaks of the profiles to an ellipse. The resulting best elliptical fit has an eccentricity of 0.65, a semi-major axis of $1.''45$, and a position angle of 289° . Based on the assumption that the intrinsic geometry of the system is circular, the inclination angle can be found, as was done by Roddier et al. (1996) and Guilloteau et al. (1999). The elliptical fit to the data suggests that the disk is inclined at 40° to our line of sight, consistent with the inclinations found under similar assumptions by Roddier et al. (1996) and Guilloteau et al. (1999).

Two consistency checks can be made on the assumption that the ring is intrinsically circular. The first test requires the position angle of the disk edge

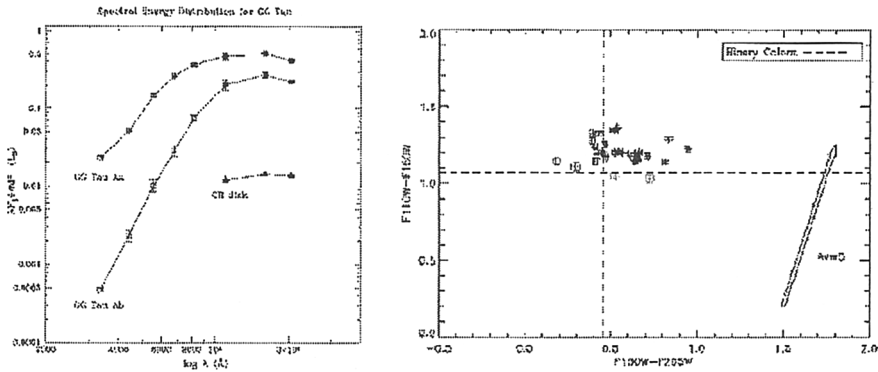


Figure 2. (a) Optical and NIR Spectral Energy Distribution for GG Tau and the circumbinary disk. 1σ error bars are plotted for each point. Open symbols refer to WFPC2 data from Ghez et al. (1997), filled symbols are from this work. (b) Color-color diagram of the circumbinary disk, created by placing independent apertures across the disk. The reddening vectors are from Rieke and Lebofsky (1985) and show 5 mag of visual extinction. The dashed lines indicate the mean stellar color of the central binary.

that is physically closest to the line of sight, and which is consequently the brightest and thinnest region, to be 90° away from the PA of the fitted ellipse. This appears to be the case, although an offset of as much as 20° may be present. The second test checks that the position of the true focus of the disk is consistent with the center of mass of the system (assumed to be the center of mass of the binary). For a circular model, we find that the true focus is offset from the center of mass of the binary by $0.''23 \pm 0.01$. The observed offset from the center of mass of the binary may partly be due to geometric effects from viewing an inclined ring in scattered light, where the edge closest to us appears closer to the central stars than it really is. Such an effect will shift the true focus from the center of mass along the semi-minor axis of the disk. However, the observed position of the true focus is significantly off this line and therefore this geometric effect, while probably occurring, does not account for the entire offset. One possible explanation is that the ring is intrinsically non-circular due to dynamical interactions with the central binary star (e.g., Artymowicz & Lubow, 1994).

3. Disk Photometry

The flux density of the circumbinary disk, which covers $\sim 13 \text{ arcsec}^2$, and that of the central stars are shown in Figure 2a. The disk appears to re-process $\sim 1.5\%$ of the stellar light in each filter.

The overall disk color excesses can be found by comparing the disk flux densities to those of the binary system. We find that the disk is *redder* than the central stars for both color indices.

$$E(F110W-F160W) = 0.08 \pm 0.02$$

$$E(F160W-F205W) = 0.17 \pm 0.05$$

These red color excesses are different from those found by Roddier et al., but are nevertheless consistent to within 2σ due to the large uncertainties in the earlier results. The more precise colors, however, do not alleviate the problem of the observed red colors; scattered light is expected to be either blue or neutral compared to the input spectrum, not redder.

Reddening of the starlight prior to scattering can play an important role, as Wood et al. (1999) demonstrated in modeling the Roddier et al. (1996) results. However, in this disk model the excess decreases with wavelength whereas the NICMOS results show excesses that increase with wavelength. It is possible that a population of large dust particles within the disk cause the observed red excess.

The picture becomes more complicated when the spatially resolved disk colors are considered. Significant changes in color are seen across the surface of the disk (see Figure 2b). The scatter of disk colors around the stellar color are inconsistent with ISM scattering. From reddening, one would expect to see less scatter in F160W-F205W than in F110W-F160W. We find that the scatter in color is a factor of 2 larger at longer wavelengths. This more detailed investigation of the disk colors, made possible by the high resolution and dynamic range of the NICMOS observations, show that while extinction may be present, it alone is not responsible for the unusual colors observed. The color variations within the disk may be indicative of inhomogeneities in the disk properties.

Acknowledgments. The authors would like to thank Mike Jura for his insightful comments. This research was based on observations made with the NASA/ESA Hubble Space Telescope, obtained at the Space Telescope Science Institute. Support for this work was provided by NASA through grant number GO-06735.01-95A from the Space Telescope Institute, which is operated by the Association of Universities for Research in Astronomy, Inc., under NASA contract NAS5-26555. CM also wishes to thank the NASA AstroBiology Institute (NABI) for supporting this work.

References

- Artymowicz, P., & Lubow, S. 1994, *ApJ*, 421, 651
Bertout, C., Robichon, N., & Arenou, F. 1999, *A&A*, 352, 574
Dutrey, A., Guilloteau, S., & Simon, M. 1994, *A&A*, 286, 149
Ghez, A. M., Neugebauer, G., & Matthews, K. 1993, *AJ*, 106, 2005
Ghez, A. M. et al. 1995, *AJ*, 110, 753
Ghez, A. M., White, R., & Simon, M. 1997, *ApJ*, 490, 353
Guilloteau, S., Dutrey, A., & Simon, M. 1999, *A&A*, 348, 570
Rieke, G., & Lebofsky, M. J. 1985, *ApJ*, 288, 618
Roddier, C. et al. 1996, *ApJ*, 463, 326
Simon, M., & Guilloteau, S. 1992, *ApJ*, 397, L47
White, R., Ghez, A. M., Reid, N., & Schultz, G. 1999, *ApJ*, 520, 811
Wood, K., Crosas, M., & Ghez, A. M. 1999, *ApJ*, 516, 335